

# Phase mixing in time-independent Hamiltonian systems

Henry E. Kandrup\*

*Departments of Astronomy and Physics and Institute for Fundamental Theory, University of Florida, Gainesville, Florida 32611*

(Accepted 1998 . Received 1998 ; in original form 1998 )

## ABSTRACT

This paper describes the evolution of localised ensembles of initial conditions in two- and three-dimensional time-independent potentials which admit a coexistence of regular and chaotic orbits. The coarse-grained approach towards an invariant, or near-invariant, distribution was probed by tracking (1) moments  $\langle x^i y^j z^k p_x^l p_y^m p_z^n \rangle$  for  $i+j+k+l+m+n \leq 4$  and (2) binned representations of reduced distributions  $f(Z_a, Z_b)$  for  $a \neq b = x, y, z, p_x, p_y, p_z$  computed at fixed intervals  $\Delta t$ . For ensembles of “unconfined” chaotic orbits in two-dimensional systems not stuck near islands by cantori, the moments evolve exponentially. Quantities like the dispersion  $\sigma_{px}$ , which start small and eventually asymptote towards a larger value, initially grow exponentially in time at a rate comparable to  $\bar{\chi}$ , the mean value of the largest short time Lyapunov exponent for orbits in the ensemble. Quantities like  $|\langle p_x \rangle|$ , that can start large but eventually asymptote towards zero, decrease exponentially. With respect to a discrete  $L^p$  norm, reduced distributions  $f(Z_a, Z_b)$  generated from successive snapshots exhibit an overall exponential decay towards a near-invariant  $f_{niv}(Z_a, Z_b)$ , although a plot of  $Df(t) \equiv \|f(t) - f_{niv}\|$  can exhibit considerable structure. Implementing an additional coarse-graining by averaging over several successive snapshots can reduce the amount of structure and increase the rate  $\Lambda_{ab}$  at which ensembles asymptote towards  $f_{niv}$ . Regular ensembles behave very differently, both moments and  $Df$  evolving in a fashion better represented by a power law time dependence. “Confined” chaotic orbits, initially stuck near regular islands because of cantori, exhibit an intermediate behaviour. The behaviour of ensembles evolved in three-dimensional potentials is qualitatively similar, except that, in this case, it is relatively likely to find one direction in configuration space which is “less chaotic” than the other two, so that quantities like  $\Lambda_{ab}$  depend more sensitively on which phase space variables one tracks.

**Key words** chaos – galaxies: formation – galaxies: kinematics and dynamics

\*E-mail: kandrup@astro.ufl.edu

## 1 INTRODUCTION AND MOTIVATION

Galactic dynamicists are interested in how, given generic initial conditions, a self-gravitating system of nearly point mass stars will evolve towards a statistical equilibrium or near-equilibrium. This question can be, and in many cases has been, formulated in the context of the full many-body problem, where the natural arena of physics is the  $6N$ -dimensional phase space. However, at least for large  $N$  it is customary to assume that the system can be characterised by a one-particle distribution function,  $F(t)$ , satisfying the collisionless Boltzmann equation, which is believed to describe the  $N$ -body problem correctly in a suitable  $N \rightarrow \infty$  limit (see, e.g., Binney & Tremaine 1987).

In this latter setting, conventional wisdom is dominated by Lynden-Bell's (1967) theory of violent relaxation, which views the evolution of the one-particle  $F$  as a phase mixing process. A mathematically rigorous analysis of this phase mixing must involve a description which incorporates the fact that the collisionless Boltzmann equation is an infinite-dimensional Hamiltonian system, with  $F$ , the fundamental dynamical variable, evolving in the infinite-dimensional phase space of distribution functions (see, e.g., Morrison 1980, Kandrup 1998, and references contained therein). However, dating back at least to Lynden-Bell's original paper (cf. his balls rolling in a pig-trough), there has been the expectation that the qualitative character of the approach towards a statistical equilibrium, i.e., a time-independent solution to the collisionless Boltzmann equation, can be understood heuristically in the context of a much simpler toy problem, namely a one-particle distribution function evolved in a fixed time-independent potential.

This seems quite reasonable. However, the question then arises as to whether that potential is integral or near-integrable, so that (almost) all the orbits are regular, or whether instead it is far from integrable, so that the phase space admits a coexistence of large measures of both regular and chaotic orbits. If the orbits are all regular, as was implicit in Lynden-Bell's original discussion, any tendency for  $F$  to evolve towards an equilibrium should be relatively weak. In particular, one might expect that, as probed by the behaviour of coarse-grained distribution functions or various moments associated with  $F$ , any approach towards equilibrium will proceed as a power law in time. By contrast, if the initial  $F(t_0)$  samples a phase space region where all the orbits are chaotic, one might expect a much more efficient evolution towards a (near-)equilibrium, the approach now proceeding exponentially in time.

The objective of the research described in this paper was to understand the bulk properties of flows in a complex time-independent potential which admits a coexistence of significant measures of both regular and chaotic orbits. Is it, for example, true that ensembles of chaotic orbits exhibit exponential phase mixing, whereas regular ensembles exhibit a more modest power law phase mixing? This is a problem of obvious interest in its own right. However, this work should also be understood as a prolegomena to a more complete treatment of violent relaxation which will generalise this work in two important ways, namely by allowing for self-consistency (Habib, Kandrup, Pogorelov, & Ryne 1998) and discreteness effects (Pogorelov & Kandrup 1998). To assess the importance of self-consistency and discreteness effects, one first needs to understand what happens when these complications are completely ignored.

Self-consistency must eventually be incorporated because the collisionless Boltzmann equation describes an evolution in response to a self-consistently determined potential. Although less obvious, discreteness effects could also play an important role. Indeed, numerical computations have shown that even very weak friction and noise, which are often used to

model discreteness effects (see, e.g., Chandrasekhar 1943), can have significant evolutionary effects on a surprisingly short time scale (Habib, Kandrup, & Mahon 1997, 1998, Kandrup 1999) by facilitating diffusion through cantori (Aubry & Andre 1978, Mather 1982) or along an Arnold web (Arnold 1964).

The numerical experiments described here involved specifying an initial distribution,  $F(\mathbf{r}, \mathbf{p}, t_0)$ , localised in a small phase space region, and understanding how  $F$  changes when evolved into the future. In particular, is there an efficient approach towards an invariant, or near-invariant, distribution? As a practical matter, this was done by (1) sampling  $F(t_0)$  to obtain a set of initial conditions, (2) integrating these initial conditions into the future, and then (3) analysing the orbits to extract systematic trends.

In this analysis two specific diagnostics played an important role:

1. *Coarse-grained reduced distribution functions.* Obtaining a high resolution numerical representation of the full four- or six-dimensional distribution function is very expensive computationally. Even in four dimensions, generating enough orbits to justify a matrix with as many as 40 cells on a side is very time-consuming, except on the very fastest computers. Indeed, such a matrix would contain  $2.56 \times 10^6$  cells, so that even storing the data for a large number of snapshots would be a nontrivial concern. For this reason, attention here focused on reduced two-variable distributions  $f(Z_a, Z_b)$ , with  $Z_a \neq Z_b = x, y, z, p_x, p_y, p_z$ , the obvious question being whether such reduced  $f$ 's evolve towards a time-independent form and, if so, how this evolution proceeds in time.

2. *Moments of the four- or six-dimensional distribution function.* Following a set of moments, even working up to relatively high order, entails tracing a relatively small collection of numbers, rather than phase space functions, and is thus comparatively inexpensive. Moreover, moments are often easily related to observables, so that a knowledge of their form allows one to determine whether, in terms of real, measureable quantities, orbit ensembles evolve towards a time-independent state.

As stressed already, one crucial issue in all this is: how does the qualitative character of the flow depend on whether the initial  $F(t_0)$  probes phase space regions characterised by regular or chaotic orbits? Even considering only chaotic initial conditions, one might expect to see very different sorts of behaviour. For example, in two-dimensional Hamiltonian systems one anticipates important distinctions between confined, or sticky, regions (cf. Contopoulos 1971), corresponding to orbits initially trapped by cantori near regular islands, and unconfined, or nonsticky, regions with orbits that move relatively unimpeded through large portions of the chaotic regions far from any regular island. However, the average divergence of nearby trajectories is set by various short time Lyapunov exponents, the typical values of which will differ for sticky and non-sticky regions (Mahon, Abernathy, Bradley, & Kandrup 1995), so that one might expect correlations between the values of short time Lyapunov exponents and the bulk properties of initially localised orbit ensembles.

Earlier work by Kandrup & Mahon (1994) and Mahon, Abernathy, Bradley, & Kandrup (1995) provided some tentative conclusions about two-dimensional Hamiltonian systems. For example, it was found that, with respect to a discrete  $L^1$  form, binned distributions  $f(x, y)$  and  $f(p_x, p_y)$  associated with chaotic ensembles of fixed energy typically exhibit a coarse-grained, exponential approach towards a near-invariant distribution  $f_{niv}$  at a rate  $\Lambda$  that correlates with  $\bar{\lambda}$ , the mean positive short time Lyapunov exponent for the ensemble. This distribution is near-invariant in the sense that, once achieved, it only changes on significantly longer times. However,  $f_{niv}$  does not in general correspond to a *true* invariant distribution  $f_{iv}$ . When integrated for much longer times,  $f$  changes as orbits slowly diffuse

through cantori to access regions that were avoided systematically over shorter time scales. The *true* invariant distribution, which  $f$  may approach only at very late times, corresponds to a microcanonical equilibrium, i.e., a uniform (in canonical coordinates) population of those phase space regions on the constant energy surface that are accessible to the ensemble.

That earlier work involved three distinct coarse-grainings, namely: (i) considering reduced distributions  $f(Z_a, Z_b)$ , rather than the full  $F$ ; (ii) considering binned representations of  $f$ ; and (iii) averaging over several successive snapshots (this to reduce the number of orbits to be computed!). Coarse graining *per se* is not a bad idea since, given Liouville’s Theorem, there can be no pointwise approach towards a time-independent equilibrium. However, one may wonder whether both temporal and phase space coarse grainings are necessary. In particular, it would seem important to determine whether the conclusions of Kandrup & Mahon (1994) remain valid in the absence of any temporal coarse graining. The first two coarse-grainings are reasonable physically in analysing experimental data where, at a fixed moment in time, one makes a measurement of some specific observable with finite phase space resolution. Temporal coarse-grainings would seem less well motivated physically. Another obvious question, as yet unanswered, is whether, for a given ensemble, the convergence rate  $\Lambda_{ab}$  is the same for different reduced distributions  $f(Z_a, Z_b)$ . Different choice of variables could lead to different values of  $\Lambda_{ab}$  since, in general, the initial ensemble could “mix” at different rates in different directions.

Merritt & Valluri (1996) subsequently exploited techniques similar to those developed by Kandrup & Mahon (1994) and Mahon, Abernathy, Bradley, & Kandrup (1995) to conclude that, in at least some three-dimensional potentials, ensembles of chaotic initial conditions will again exhibit an exponential approach towards a near-invariant  $f_{niv}$ . Unlike earlier work on two-dimensional systems, that paper did not implement a temporal coarse-graining. However, the authors probed the approach towards  $f_{niv}$  using a diagnostic which yields no information about direction-dependence, so that they could not address the possibility of “mixing” at different rates in different directions. Moreover, none of the earlier work on either two- or three-dimensional flows has addressed the question of how the lower order moments evolve in time.

To a large extent, these moments divide into two types, namely (1) those like  $\sigma_{px}$ , the dispersion in  $p_x$ , which start small and presumably asymptote towards a larger nonzero value, and (2) those like the mean  $\langle p_x \rangle$  which typically start with a finite value but, at least for chaotic ensembles, would be expected to evolve towards zero. It seems reasonable to conjecture that, for moments of the first type, chaotic ensembles exhibit an initial growth that is exponential in time, whereas regular ensembles exhibit a slower, power law growth. Alternatively, one might anticipate that moments like  $\langle p_x \rangle$  will decay to zero exponentially for chaotic ensembles but – if at all – only much more slowly for regular ensembles.

Section 2 describes the behaviour of moments and reduced distributions extracted from an analysis of orbits in two-dimensional potentials. Section 3 then discusses how these results are changed by allowing for a three-dimensional potential. Section 4 concludes by summarising the principal results and commenting on their significance.

## 2 TWO-DIMENSIONAL SYSTEMS

### 2.1 Description of what was computed

The conclusions described in this Section derive from a study of three different Hamiltonian

systems of the form

$$H = \frac{1}{2}(p_x^2 + p_y^2) + V(x, y). \quad (1)$$

The potentials that were used included the sixth order truncation of the Toda (1967) potential, namely

$$V(x, y) = \frac{1}{2}(x^2 + y^2) + x^2y - \frac{1}{3}y^3 + \frac{1}{2}x^4 + x^2y^2 + \frac{1}{2}y^4 \\ + x^4y + \frac{2}{3}x^2y^3 - \frac{1}{3}y^5 + \frac{1}{5}x^6 + x^4y^2 + \frac{1}{3}x^2y^4 + \frac{11}{45}y^6; \quad (2)$$

the sum of isotropic and anisotropic softened Plummer potentials, namely (Mahon, Abernathy, Bradley, & Kandrup 1995)

$$V(x, y) = -\frac{1}{(c^2 + x^2 + y^2)^{1/2}} - \frac{m}{(c^2 + x^2 + ay^2)^{1/2}}, \quad (3)$$

with  $c = 20^{2/3} \approx 0.136$ ,  $a = 0.1$  and  $m = 0.3$ ; and the so-called dihedral potential of Armbruster, Guckenheimer, & Kim (1989) for one particular set of parameter values, namely

$$V(x, y) = -(x^2 + y^2) + \frac{1}{4}(x^2 + y^2)^2 - \frac{1}{4}x^2y^2. \quad (4)$$

Although these potentials manifest very different symmetries, the basic conclusions about the evolution of orbit ensembles are very similar, which suggests that they are robust. Because of this similarity, the discussion here focuses primarily on the dihedral potential which, being the most inexpensive to implement computationally, could be explored for the largest number of orbits, thus yielding results of the greatest statistical significance.

Each experiment involved an ensemble of  $81 \times 81 = 6561$  initial conditions with the same fixed energy  $E$ . In general, different ensembles were chosen to sample only regular or only chaotic orbits, as identified using a surface of section. These were generated by uniformly sampling a square in the  $y - p_y$  plane, typically with sides  $\Delta y = \Delta p_y = 0.2$ , setting  $x = 0$ , and solving for  $p_x = p_x(y, p_y, E) > 0$ . A Burlisch-Stoer or fourth order Runge-Kutta integrator was used to evolve each initial condition for  $t \geq 256$ , a time corresponding to an interval of order 100 – 200 crossing times  $t_{cr}$ . The integrator solved simultaneously for the evolution of a small, linearised perturbation, renormalised at fixed intervals  $\Delta t = 1.0$ , so as to obtain an estimate of the largest Lyapunov exponent  $\chi$  (see, e.g., Lichtenberg & Lieberman 1992). The phase space coordinates and short time  $\chi$  were recorded for each orbit at intervals  $\Delta t = 0.25, 0.5$ , or  $1.0$ . Most of the analysis focused on ensembles of chaotic orbits, which were expected to exhibit the most interesting behaviour.

Each ensemble of initial conditions was interpreted as sampling an initial distribution  $F(x, y, p_x, p_y, t_0)$ , and the evolved orbits were interpreted as yielding an approximation to the true  $F(t)$  associated with the initial  $F(t_0)$ . The data were thus binned to yield  $n \times n$  coarse-grained gridded approximations of the six possible reduced two-dimensional distributions  $f(Z_a, Z_b, t)$  with  $a \neq b = x, y, p_x, p_y$ . Most of the analysis involved the choice  $n = 20$ . It was verified that  $n = 10, 30$ , and  $40$  yielded no differences that could not be attributed to finite number statistics.

The expected coarse-grained approach towards equilibrium associated with chaotic ensembles was probed in two distinct ways. The first involved determining how, with respect to an appropriate norm, the coarse-grained distributions  $f(t)$  evolve towards an invariant,

or near-invariant,  $f_{inv}$ . Consistent with earlier experiments (Kandrup & Mahon, 1994, Mahon, Abernathy, Bradley, & Kandrup 1995), it was observed that, after a relatively short interval, the orbit ensembles typically evolved towards a state which is near-invariant in the sense that, once attained, it only exhibits large systematic shifts on a much longer time scale. Physically, this state seems to correspond to a near-constant population (in canonical coordinates) of those portions of the constant energy hypersurface that are easily accessible to the orbits, i.e., not blocked by relatively impenetrable cantori. The evolution observed at much later times involves orbits diffusing through cantori to probe regions on the constant energy surface that were avoided systematically on short time scales (cf. MacKay, Meiss, & Percival 1984). Approximations to the near-invariant distributions  $f_{niv}(Z_a, Z_b)$  were generated by averaging over orbital data generated from 64 successive snapshots at intervals  $\Delta t = 1.0$ , usually extending from  $t = 193$  to  $t = 256$  but, when convergence was slow, from a significantly later interval. The approach of  $f(t)$  towards  $f_{niv}$  was quantified by tracking the “distance” between  $f(t)$  and  $f_{niv}$ , as defined by the discrete  $L^p$  norm

$$Df(Z_a, Z_b, t) = \left( \frac{\sum_a \sum_b |f(Z_a, Z_b, t) - f_{niv}(Z_a, Z_b)|^p}{\sum_a \sum_b |f_{niv}(Z_a, Z_b)|^p} \right)^{1/p}, \quad (5)$$

with  $p = 1$  or  $2$ .

The orbital data were also used to track the evolution of all possible moments  $\langle x^i y^j p_x^k p_y^l \rangle$  with non-negative integers  $i + j + k + l \leq 4$ . One can view these moments either directly as probes of the 6561-orbit ensemble or as probes of statistics of the smooth phase space distribution  $F(x, y, p_x, p_y, t)$ . The latter viewpoint suggests that one might expect correlations between the way in which  $f(t)$  evolves towards  $f_{niv}$  and the way in which such moments as  $\langle p_x \rangle$  evolve towards zero. In particular, if  $Df(t) \rightarrow 0$  exponentially, one might expect that  $\langle p_x(t) \rangle \rightarrow 0$  as well. Alternatively, the systematic divergence of nearby initial conditions exhibited by chaotic orbits would suggest that, for an initially localised ensemble, quantities like  $\sigma_{p_x}(t)$  should *grow* exponentially at early times.

## 2.2 Convergence towards a near-invariant distribution $f_{niv}$

Consider first the evolution of the six reduced distributions  $f(Z_a, Z_b)$  without any temporal averaging. Here one finds that, for ensembles of initial conditions corresponding to unconfined chaotic orbits, i.e., chaotic orbits not trapped by cantori near regular islands, there is a coarse-grained approach towards a near-invariant distribution  $f_{niv}$  which, when quantified in terms of either an  $L^1$  or  $L^2$  norm, proceeds exponentially in time, i.e.,  $Df(t) \propto \exp(-\Lambda t)$ . At very early times, when  $f$  has nonvanishing support only in a small number of cells, plots of the  $L^1$ - and  $L^2$ - distances can differ significantly, the  $L^2$ -distance starting larger but decreasing substantially more quickly. However, once the initial ensemble has spread out so as to have nonzero support in a significant fraction of the cells, the  $L^1$  and  $L^2$  rates agree, at least approximately. This suggests that the rate of convergence towards a near-invariant  $f_{niv}$  is insensitive to the detailed choice of norm, a result that was confirmed by exploring the effects of allowing for other  $L^p$  norms. In all cases, the rate  $\Lambda$  corresponds to a time scale  $\tau \equiv \Lambda^{-1}$  which is comparable to, albeit somewhat longer than a characteristic crossing time  $t_{cr}$ . In other words, the approach towards a near-invariant  $f_{niv}$  proceeds on the natural time scale  $t_{cr}$  or, equivalently, the time scale  $\chi^{-1}$  on which small perturbations in initial conditions would be expected to grow.

This behaviour is illustrated in Fig. 1. Here panel (a) exhibits the  $L^1$  and  $L^2$  distances  $Df(x, y)$  for an ensemble of unconfined chaotic orbits with energy  $E = 1.0$  evolved in the

dihedral potential. At very early times, the remaining five distances,  $f(x, p_x)$ ,  $f(x, p_y)$ ,  $f(y, p_x)$ ,  $f(y, p_y)$  and  $f(p_x, p_y)$ , not shown, look different from both  $f(x, y)$  and each other but, after a time  $t \sim 10$  they exhibit similar curvatures. In each case,  $Df$  decreases exponentially until a time  $\sim 40$ , and then asymptotes towards a near-constant value. This later time behaviour is a finite size effect. Neither the near-invariant  $f_{niv}$  nor the true time-dependent  $f(t)$  is determined exactly, since each was generated from a finite number of orbits, so that, even if the computed  $f(t)$  and  $f_{niv}$  both sample the *true*  $\hat{f}_{niv}$ , the distance  $Df$  between them will not vanish exactly. Fig. 1 (b) exhibits the corresponding  $L^1$ - and  $L^2$ -distances for a chaotic ensemble with  $E = 6.0$  again evolved in the dihedral potential. Once more the decay of all the  $Df$ 's is exponential, but the convergence rates  $\Lambda_{ab}$  are substantially smaller, so that  $Df$  continues to decrease until  $t \sim 100$ .

Initially localised ensembles of regular orbits, for which all the Lyapunov exponents vanish identically, disperse much less efficiently. To the extent that any approach towards a near-invariant  $f_{niv}$  is observed, it will proceed as a power law in time, and the characteristic time scale is typically long compared with the natural crossing time  $t_{cr}$ .

Ensembles corresponding to chaotic orbits originally confined near regular islands by cantori behave somewhat differently. Once again there is an approach towards a near-invariant  $f_{niv}$  which, in many cases, is reasonably well fit by an exponential (although a power law fit often proves nearly as good!). However the rates  $\Lambda$  tend to be significantly smaller than the rates associated with unconfined ensembles with the same energy. This correlates with the fact that the largest short time Lyapunov exponent (see, e.g., Grassberger, Badii, & Politi 1988) for a confined chaotic segment, albeit nonzero, is typically much smaller than the largest short time exponent for an unconfined segment with the same energy (Mahon, Abernathy, Bradley, & Kandrup 1995). Figs. 1 (c) and (d) exhibit the distances  $Df(x, p_x)$  and  $Df(y, p_y)$  for an ensemble of confined chaotic orbits with  $E = 6.0$ . Here decreases in the  $Df$ 's are reasonably well fit by an exponential, but it is clear that the rates  $\Lambda_{ab}$  are much smaller than those associated with the ensemble from which Fig. 1 (b) derives.

The near-invariant  $f_{niv}$  associated with an ensemble of confined chaotic orbits is typically very different from the  $f_{niv}$  associated with an unconfined ensemble, avoiding as it does large portions of the stochastic sea far from any regular islands. If the initial conditions be integrated for a sufficiently long time, often  $t \sim 1000$  or more, the resulting orbits eventually diffuse through cantori to probe these depths of the stochastic sea and approach a true invariant distribution. Ensembles of initially unconfined chaotic orbits also exhibit diffusion through cantori on a comparable time scale as some fraction of the orbits become trapped near regular islands. However, this is usually a much less conspicuous effect since, at least for the three potentials considered here, the volume of the confined chaotic regions is typically much smaller than the volume of the unconfined chaotic region.

When probing the initial approach towards a near-invariant  $f_{niv}(Z_a, Z_b)$  exhibited by an ensemble of unconfined chaotic orbits, it is also useful to quantify the degree to which the best fit rate  $\Lambda_{ab}$  is approximately the same for all six choices of reduced distribution. In most cases, the answer appears to be: yes. If best fit slopes are extracted for all six possibilities and their values compared, one typically finds agreement at the 5 – 10% level. However, one *does* see occasional exceptions where, compared with the remaining  $\Lambda$ 's, one of the  $\Lambda_{ab}$ 's is especially small and another is especially large. In virtually every case, the exceptional distributions are  $f_{niv}(x, p_x)$  and  $f_{niv}(y, p_y)$ . Physically, an especially small  $\Lambda_{xpx}$  and an especially large  $\Lambda_{ypy}$  corresponds to a flow in which, when viewed in configuration

space, initially proximate orbits tend to diverge much more quickly in the  $x$ -direction than in the  $y$ -direction, which implies in turn larger divergences in the  $p_x$  than the  $p_y$  direction. It follows that, respectively,  $f(x, p_x, t)$  and  $f(y, p_y, t)$  approach near-invariant distributions somewhat faster and slower than the remaining four reduced distributions which involve one fast and one slow variable. Figs. 1 (a) and (b) correspond to ensembles where all six rates are comparable. Fig. 1 (c) and (d) corresponds to an ensemble where  $\Lambda_{xpx}$  is especially small and  $\Lambda_{ypy}$  is especially large.

Another significant point is that, modulo the aforementioned examples of especially fast and slow convergences, which depend rather sensitively on the choice of ensemble, the convergence rates for different ensembles of chaotic orbits with the same energy tend to be quite similar. Specifically, to the extent that orbit segments in different ensembles yield distributions of short time Lyapunov exponents that are very similar, they may be expected to yield convergence rates that are nearly the same. However, small, but statistically significant, differences between the distributions of short time Lyapunov exponents can be observed for different chaotic ensembles, even two ensembles with the same energy both comprised entirely of unconfined chaotic orbits; and these differences, which manifest the fact that the detailed chaotic behaviour is slightly different, can translate into significant differences in the rates at which the ensembles evolve towards near-invariant  $f_{niv}$ 's.

When comparing ensembles of unconfined chaotic orbits with different energies, one also finds that, overall, the observed rates of convergence  $\Lambda$  correlate reasonably well with the mean value  $\bar{\chi}$  of the largest short time Lyapunov exponent in the sense that increases in  $\Lambda$  coincide with increases in  $\bar{\chi}$ . However, the ratio  $\mathcal{R} = \Lambda / \langle \chi \rangle$  does not always seem to assume a constant value, as was found in many cases by Kandrup & Mahon (1994) when considering reduced distributions  $\tilde{f}(Z_a, Z_b)$  that averaged over several successive time steps.

Finally, it should be noted that, in addition to everything else, a plot of  $Df(t)$  can exhibit considerable structure superimposed on the exponential approach, the details of which depend on (i) which reduced distribution one considers, (ii) which energy (and class of chaotic orbit) that one probes, and even (iii) which specific ensemble of initial conditions one chooses. The fact that, overall,  $Df(t)$  decays to zero exponentially is a robust statement but, as noted, e.g., by Merritt & Valluri (1996), it does not constitute the whole story. An extreme example of this is exhibited in Fig. 1 (e) and (f), which exhibit two of the  $Df$ 's for an ensemble of unconfined chaotic orbits with  $E = 4.0$  evolved in the dihedral potential. For this and most other ensembles,  $Df(x, p_x)$  and  $Df(y, p_y)$  exhibit relatively little structure superimposed on their exponential decrease, whereas the four remaining  $Df$ 's exhibit larger amplitude oscillations. (Similar  $Df(x, y)$ 's can also be observed when one performs Langevin simulations, generating multiple realisations of single initial condition evolved in the presence of low amplitude friction and noise, and tracks the evolved ensemble of orbits as it approaches a near-invariant distribution (see, e.g., Fig. 7 in Habib, Kandrup, & Mahon 1997).

The results described hitherto all pertain to the behaviour of individual snapshots, without any temporal coarse-graining. However, it is also interesting to determine what happens if instead one considers a coarse-grained  $\tilde{f}(Z_a, Z_b, t)$  which averages over several successive time steps. This was explored for the potentials (2) - (4) by analysing data recorded at various intervals between  $\Delta t = 0.25$  and  $\Delta t = 2.0$ , which were averaged over  $k$  successive time steps. An investigation of the effects of increasing  $k$  facilitated two concrete conclusions:

1. As probed by the  $L^1$  distance, averaging over several successive snapshots leads gener-

ically to a significant increase in the rate at which an ensemble evolves towards a near-invariant distribution. By contrast, averaging has a comparatively minimal effect on the computed  $L^2$  distance. For this reason the  $L^1$  and  $L^2$  convergence rates  $\lambda_{ab}$  associated with data averaged over successive snapshots are in better agreement than the unaveraged rates  $\Lambda_{ab}$ , although the  $L^1$  rates tend to remain somewhat smaller.

2. The exact number of time steps over which one averages is relatively unimportant. Assuming that snapshots are recorded at intervals  $\Delta t \sim t_{cr}$ , averages over different  $k$ 's extending from  $5 < k < 25$  lead relatively similar results; and, similarly, varying  $\Delta t$  from  $\sim 0.25t_{cr}$  to  $2.0t_{cr}$  has a comparatively minor effect.

A concrete example of this behaviour is shown in Fig. 2, which plots the  $L^1$  and  $L^2$  distances  $D\tilde{f}(x, y, t)$  computed for the same ensemble of unconfined chaotic orbits used to generate Fig. 1 (a). This Figure was generated by recording data at intervals  $\Delta t = 0.5$  and then averaging over  $k = 3$  and 15 time steps, corresponding to intervals extending from  $\Delta T = 1.5$  to  $\Delta T = 7.5$ . The specific value associated with time  $t$  involves an average from times  $t$  to  $t + 0.5k$ . Overall, the  $L^1$  slopes associated with  $5 < k < 25$  are similar to one another and somewhat larger in magnitude than that slopes for  $1 \leq k \leq 3$  (the value  $k = 1$  corresponds to Fig. 1(a)). By contrast, the  $L^2$  slopes for  $1 \leq k \leq 3$  do not differ substantially from the slopes computed with larger  $k$ .

Overall, comparing different values  $5 \leq k \leq 25$  for a single ensemble with the same reduced  $\tilde{f}(Z_a, Z_b)$  yields agreement at the 4 – 8% level. Comparing the mean  $\lambda_{ab}$  for the same ensemble but different reduced distributions typically yields agreement at the 2 – 4% level (except for the aforementioned exceptional cases where one  $\Lambda_{ab}$  is especially large and another especially small.. Comparing the typical values of  $\Lambda_{ab}$  and/or  $\lambda_{ab}$  for different ensembles with the same energy indicates that, when the mean short time  $\bar{\chi}$ 's are very similar, the computed  $\Lambda_{ab}$  and/or  $\lambda_{ab}$  will also coincide. Comparing the typical values of  $\Lambda_{ab}$  and  $\lambda_{ab}$  for ensembles with different energies demonstrates that there is a reasonable correlation between  $\bar{\chi}$  and both  $\Lambda_{ab}$  and  $\lambda_{ab}$ . Energies for which unconfined chaotic orbits have larger values of  $\bar{\chi}$  tend systematically to have larger values of  $\Lambda_{ab}$  and  $\lambda_{ab}$  as well.

The trends connecting  $\bar{\chi}$ ,  $\Lambda_{ab}$ , and  $\lambda_{ab}$  are exhibited in Fig. 3, which plot  $0.5\bar{\chi}$  (solid curve), the  $L^2$  rate  $\Lambda_{L2}$  for individual snapshots (dashed curve), the  $L^1$  rate  $\Lambda_{L1}$  for individual snapshots (dot dashed), and the  $L^1$  rate  $\lambda_{L1}$  generated by averaging over different coarse-grainings with  $5 < k < 25$  (triple-dot-dashed). Each  $\Lambda$  and  $\lambda$  involved averaging over all six possible reduced distributions.

### 2.3 Evolution of lower order moments

Turn now to the evolution of lower order moments, considering first quantities like  $\langle x \rangle$  which, when computed using the invariant  $F_{iv}(x, y, p_x, p_y)$  appropriate for an ensemble of chaotic orbits, vanish by symmetry. Here one finds that, for ensembles of initial conditions corresponding to unconfined chaotic orbits, such moments as  $\langle x \rangle$ ,  $\langle xy \rangle$ , or  $\langle xy^2 \rangle$  do indeed evolve towards zero, the expected result for a microcanonical sampling of the chaotic portions of the constant energy hypersurface. A plot of these decaying moments can exhibit a considerable amount of structure but, nevertheless, one finds that, in almost every case, the envelop approaches zero exponentially.

An obvious question is whether, for a given ensemble, the moments which decay to zero exponentially all do so at the same, or at least comparable, rates. The answer here is that, overall, the rates are often very similar. Consider, e.g., the linear moments  $\langle x \rangle$ ,  $\langle y \rangle$ ,  $\langle p_x \rangle$ , and  $\langle p_y \rangle$  which, for the Hamiltonians considered in this paper, should vanish when evaluated

for an  $E = \text{constant}$   $F_{iv}(x, y, p_x, p_y)$ . For those energies where the phase space is relatively simple and obstructions like cantori play a relatively minimal role, the inferred rates for these moments are nearly identical, agreeing at the 5 – 10% level. However, for energies where the phase space is more complicated the moments associated with one direction, either  $x$  or  $y$ , can exhibit a much slower approach towards equilibrium, the rate  $\Gamma$  being less than half as large. The ensembles where this behaviour is observed are precisely those for which, as described in § 2.2, one  $Df(Z_a, Z_b, t)$  decays especially slowly and another especially fast.

Quadratic cross moments like  $\langle xy \rangle$  or  $\langle xp_y \rangle$  and cubic moments like  $\langle x^3 \rangle$ ,  $\langle xy^2 \rangle$  or  $\langle xyp_x \rangle$  also tend to decay at comparable rates. However, there is a slight tendency, not manifested in all cases, for some pairs e.g.,  $\langle xp_x \rangle$  or  $\langle yp_y \rangle$ , to decay somewhat slower than the other quadratic moments, which reflects the fact that correlations between a coordinate and its conjugate momentum tend to decay comparatively slowly. In addition, plots of the nonlinear moments tend to exhibit more structure than do plots of the linear moments.

This behaviour is illustrated in Fig. 4, which exhibits moments generated from the same ensemble of orbits in the dihedral potential with  $E = 1.0$  which was used to generate Fig. 1 (a). Panel (a) - (e) exhibit, respectively, one representative linear and four quadratic moments. Most of the moments decay at comparable rates, although  $\langle xp_x \rangle$  and  $\langle yp_y \rangle$  (the latter not shown) clearly decay substantially more slowly than the other quadratic moments.

Another obvious question is whether the rates associated with the decay towards zero are the same for different orbit ensembles with the same energy. Here the answer is that, overall, the rate (or largest rate, if several widely disparate rates are observed) is comparatively insensitive to the choice of ensemble, provided that one restricts attention to unconfined chaotic orbits. This largest rate typically ranges between 1/3 and 2/3 the value of  $\bar{\chi}$ , the mean largest short time Lyapunov exponent associated with the orbit ensemble, which implies a value intermediate between the rates  $\Lambda_{L1}$  and  $\Lambda_{L2}$  associated with the  $L^1$  and  $L^2$  convergence of  $f(Z_a, Z_b, t)$  towards  $f_{niv}$ .

Moments generated from ensembles of regular initial conditions evolve very differently. For regular ensembles, the moments show no evidence of an exponential decay on a time scale  $\sim \chi^{-1}$ . In general, the moments will not decay towards zero and, even if they do, the decay is much better fit by a slow power law than by an exponential.

Now consider combinations of moments like the dispersion  $\sigma_x = \sqrt{\langle x^2 \rangle - \langle x \rangle^2}$  which, for a localised ensemble of initial conditions, start small but eventually grow large. For ensembles of unconfined chaotic orbits, such quantities typically grow exponentially in time until they become “macroscopic,” so that, e.g., the magnitude of  $\sigma_x$  becomes comparable to the linear size of the configuration space region accessible to orbits with the specified energy. Moreover, one usually finds that all four dispersions,  $\sigma_x$ ,  $\sigma_y$ ,  $\sigma_{px}$ , and  $\sigma_{py}$ , grow at similar rates which are comparable to, but somewhat larger than, the mean short time exponent  $\bar{\chi}$  for the ensemble. By contrast, when evaluated for ensembles comprised of regular orbits, quantities like  $\sigma_x$  grow only much more slowly in a fashion reasonably well fit by a power law with an index  $p$  of order unity, i.e.,  $\sigma_x \propto t^p$  with  $p \sim 1.0$ . Ensembles comprised of confined chaotic orbits typically exhibit an intermediate behaviour. The typical behaviour of the dispersions for ensembles of unconfined chaotic orbits is illustrated in Fig. 5, which was again generated for the orbit ensemble with  $E = 1.0$  used to create Fig. 1.

The aforementioned behaviour for the growing modes is easy to understand: If the ensemble is chaotic, there is a systematic tendency for nearby trajectories to diverge at a rate set by the largest Lyapunov exponent for individual orbits. That the growth rate

for the dispersion is larger than  $\bar{\chi}$  reflects the obvious fact that this rate is dominated by those orbits that are most unstable. Differences between the growth rates in different directions can be attributed to the fact that, on the average, orbits in the ensemble will be exponentially unstable at somewhat different rates in different directions. If, alternatively, the orbits are regular, nearby trajectories only diverge as a power law in time, so that the dispersions exhibit a much slower power law growth. It should also be noted that the same qualitative behaviour arises when tracking the evolution of multiple realisations of the same initial condition integrated in the presence of low amplitude friction and noise (see, e.g., Habib, Kandrup, & Mahon 1997). There once again the Lyapunov exponent sets the time scale (if any) on which different orbits in the ensemble diverge exponentially, the average rate of divergence being somewhat larger than the mean  $\bar{\chi}$ .

Finally it may be noted that growing moments can be combined in interesting ways to yield quantities that decay exponentially in time. Thus e.g., one finds that  $Dx \equiv \langle x^4 \rangle - 2\langle x^2 \rangle^2$  and  $Dy \equiv \langle y^4 \rangle - 2\langle y^2 \rangle^2$  both decay towards values that are very close to zero. This exponential decay is illustrated in Fig. 4 (f), which exhibits  $\ln Dx$  for the orbit ensemble used to generate Fig. 1 (a).

### 3 THREE-DIMENSIONAL SYSTEMS

#### 3.1 Description of what was computed

The conclusions described in this Section derive from a study of Hamiltonian systems of the form

$$H = \frac{1}{2}(p_x^2 + p_y^2 + p_z^2) + V(x, y, z), \quad (6)$$

with

$$V(x, y, z) = -(x^2 + y^2 + z^2) + \frac{1}{4}(x^2 + y^2 + z^2)^2 - \frac{1}{4}(x^2y^2 + ay^2z^2 + bz^2x^2), \quad (7)$$

where  $a$  and  $b$  are real-valued constants. The most symmetric choice,  $a = b = 1$ , yields the obvious three-dimensional analogue of the two-dimensional dihedral potential, which now manifests cubic, rather than square, symmetry. Selecting  $a$  or  $b \neq 1$  breaks this symmetry. For generic values of  $a$  and  $b$ , at most energies the phase space admits a coexistence of significant measures of both regular and chaotic orbits, much as for the two-dimensional dihedral potential. However, adding a third dimension seems to make the chaotic orbits somewhat less unstable in the sense that, at least for  $a = b = 1$ , the largest Lyapunov exponent for the three-dimensional system tends to be somewhat smaller than the largest exponent for two-dimensional systems (at least for relatively low energies). The special case  $a = b = 2$  leads to the partially integrable potential

$$V(x, y) = -(x^2 + y^2) + \frac{1}{4}(x^2 + y^2)^2 - \frac{1}{4}x^2y^2 + \left(\frac{1}{4}z^2 - z^2\right), \quad (8)$$

for which motion in the  $z$ -direction is decoupled from motion in the remaining  $x$ - and  $y$ -directions.

Ensembles of 6561 initial conditions were chosen in two different ways. In some cases, these were obtained by uniformly sampling a square in the  $y - p_y$  (or  $z - p_z$ ) plane, setting  $x = 0$ , selecting fixed values for  $z$  and  $p_z$  (or  $y$  and  $p_y$ ), and then solving for  $p_x > 0$ . In other cases, they were obtained by uniformly sampling a four-dimensional  $y$ - $z$ - $p_y$ - $p_z$  hypercube with sides  $\Delta y = \Delta z = \Delta p_y = \Delta p_z = 0.2$ , setting  $x = 0$ , and solving for  $p_x > 0$ . The resulting orbits were analysed much as for the two-dimensional systems described in Section

2, except that attention focused on all 15 reduced distributions  $f(Z_a, Z_b)$  and all possible moments  $\langle x^i y^j z^k p_x^l p_y^m p_z^n \rangle$  with  $i + j + k + l + m + n \leq 4$ . One major difference observed for three-, as opposed to, two-dimensional systems was that, even for  $a = b = 1$ , the time required for a chaotic ensemble to approach a near-invariant  $f_{niv}$  could be extremely long, so that obtaining a reasonable approximation to  $f_{niv}$  sometimes required integrating an orbital ensemble for times as large as  $t \sim 1000$ . In most cases, only the largest short time Lyapunov exponent was computed. However, in some cases a more complicated code (Wolf, Swift, Swinney, and Vastano 1985) was used to extract the full spectrum of exponents.

### 3.2 Convergence towards a near-invariant distribution $f_{niv}$

Overall, the behaviour exhibited by localised ensembles of initial conditions evolved in three-dimensional potentials is quite similar to that observed in two-dimensional potentials. Ensembles of chaotic orbits, not initially stuck near a regular island, typically exhibit an exponential approach towards a near-invariant distribution  $f_{niv}$  at a rate  $\Lambda$  which is comparable in magnitude to  $\bar{\chi}$ , the mean value of the largest short time Lyapunov exponent. Alternatively, ensembles of regular orbits exhibit little, if any, tendency to evolve towards a near-invariant  $f_{niv}$ .

However, there *are* some striking differences. One important difference between two- and three-dimensional systems is that, for the latter, the approach towards a near-invariant  $f_{niv}$  often proceeds at grossly different rates in different directions. Here the determining factor is *not* in general the precise values of  $a$  and  $b$  (provided one avoids the special case  $a = b = 2$ , which leads to a partially integrable system). Rather, what seems to matter more is the location of the phase space cell that was chosen to generate the initial conditions. If, e.g., one chooses an ensemble of initial conditions with relatively small values of  $|z|$  and  $|p_z|$ , this corresponding to orbits originally moving very nearly in the  $x - y$  plane, one often finds that the approach towards a near-invariant distribution in the  $z$  and  $p_z$  directions is extremely slow. This, however, does not imply that, for such ensembles, the largest short time Lyapunov exponent is especially small. Indeed, if the initial  $|z|$  and  $|p_z|$  are both sufficiently small, the largest short time  $\bar{\chi}$  for a three-dimensional system with  $a = b = 1$  will more closely approximate the largest Lyapunov exponent  $\chi$  for a two-dimensional system than the largest  $\chi$  for a three-dimensional system.

Such a direction-dependent approach towards a near-invariant  $f_{niv}$  is illustrated in Figs. 6 (a), (c), and (e). These panels, generated from a chaotic ensemble with energy  $E = 6.0$  and an initial  $z = 0.2$  and  $p_z = 0.0$ , evolved in the potential (7) with  $a = b = 1$ , exhibits three different  $L^1$  and  $L^2$  distances, namely  $Df(x, y)$ ,  $Df(z, p_x)$ , and  $Df(z, p_z)$ . For all fifteen reduced distributions  $Df(Z_a, Z_b)$ , the approach towards a near-invariant  $f_{niv}$  is exponential in time, but three significantly different rates are observed. The six  $f(t)$ 's involving only the “fast” variables  $x$ ,  $y$ ,  $p_x$ , and  $p_y$  approach  $f_{niv}$  especially quickly, whereas  $f(z, p_z, t)$ , which involves the “slow” variables  $z$  and  $p_z$ , evolves towards  $f_{niv}$  especially slowly. The remaining eight  $f(t)$ 's, which involve one fast and one slow variable, approach  $f_{niv}$  at an intermediate rate.

Not surprisingly, this direction-dependence becomes even more striking for chaotic ensembles evolved with  $a = b = 2$ , where motion in the  $z$ -direction is integrable. In this case, one finds that, irrespective of the qualitative character of motion in the remaining four phase space directions, there is no strong exponential approach towards a near-invariant distribution associated with either the  $z$  or the  $p_z$  direction. For chaotic ensembles corresponding to orbits with one positive Lyapunov exponent, one finds that the six reduced

distributions involving  $x$ ,  $y$ ,  $p_x$ , and  $p_y$  all exhibit an exponential approach towards a near-invariant  $f_{niv}$ , typically at a rate comparable to what was observed for the two-dimensional dihedral potential. However, the remaining nine reduced distributions, all of which probe the  $z$  and/or  $p_z$  direction, exhibit a much weaker tendency to approach a near-invariant  $f_{niv}$ . The quantities  $Df(Z_a, Z_b, t)$  with  $Z_a = x, y, p_x$ , or  $p_y$  and  $Z_b = z$  or  $p_z$  do exhibit modest decreases, but  $Df(z, p_z, t)$  often shows essentially no tendency to decrease.

This behaviour is illustrated in Figs. 6 (b), (d), and (f), which exhibits the same  $L^1$  and  $L^2$  distances as did Fig. 6 (a), (c), and (e), again generated for an ensemble of chaotic initial conditions with  $E = 6.0$  but now evolved with  $a = b = 2$ . These panels should be contrasted with Figs. 7 (a) and (b), which exhibit two representative  $Df$ 's computed for an ensemble of regular orbits evolved with  $a = b = 1$ . It is apparent that, as would be expected for this latter ensemble, these distances do not exhibit an efficient exponential damping, although the  $L^2$  distances can exhibit a slow, albeit systematic, decrease.

Modulo the partially integrable case  $a = b = 2$  and special initial conditions like those initially stuck near the  $x - y$  plane, one finds typically that, as for the case of two-dimensional potentials, the convergence rates  $\Lambda_{ab}$  associated with different reduced distributions  $f(Z_a, Z_b, t)$  computed for the same ensemble of chaotic orbits tend to be comparatively similar. However, a comparison of results from different ensembles exhibits more diversity than what was observed in two-dimensional systems. Indeed, when sampling different portions of a single connected phase space region, all corresponding to chaotic orbits initially located relatively far from any large regular islands, one often finds convergence rates  $\Lambda_{ab}$  that differ by substantially more than 10%. This diversity appears to correlate with the fact that different ensembles extracted from the same connected phase space region can be characterised by distributions of short time Lyapunov exponents,  $N[\chi]$ , which differ substantially more than what was observed for the corresponding distributions in two-dimensional systems.

It is also interesting to determine the effects of averaging over successive snapshots. For ensembles where the orbits behave chaotically in all three spatial dimensions, averaging over two or more successive snapshots has much the same effect as for two-dimensional systems. In particular, the  $L^1$  rate of convergence increases if one averages over two or more snapshots and, when averaged over (say) five or more snapshots, appears to asymptote towards a value  $\lambda_{ab}$  that is insensitive to the precise number  $k$  of successive time steps used to compute the average. When considering orbit ensembles that are chaotic in two directions but regular in the third, one also finds that, at least in the chaotic directions, averaging yields the same behaviour as for two-dimensional systems. However, when probing the integrable direction (if any) associated with a flow, temporal averaging has a different effect. In this case, averaging over successive time steps *can* amplify at least slightly a very weak tendency to evolve towards some  $f_{niv}$ . More important, however, is the fact that the averaging *per se* yields a  $\tilde{f}$  that more closely approximates  $f_{niv}$ , even at very early times. The reason for this is not hard to see. Because motion in the  $z - p_z$  plane is periodic, it is easy to associate a near-invariant  $f_{niv}(z, p_z)$  with even a single orbit by computing the relative amount of time that the orbit spends in the neighbourhood of each point in the  $z - p_z$  plane. The obvious point then is that if a localised ensemble of initial conditions exhibits no appreciable tendency to disperse, averaging over a sufficiently large number of successive snapshots will yield a decent approximation to  $f_{niv}$  which, for a fixed number of equally spaced snapshots, should not differ appreciably when evaluated for early and late intervals,  $t_1 < t < t_2$  and  $t_1 + T < t < t_2 + T$ .

### 3.3 Evolution of lower order moments

An examination of moments generated from ensembles evolved in three-dimensional potentials leads to two general conclusions:

1. When considering ensembles of orbits that are wildly chaotic in all three directions, one finds the same qualitative behaviour as was observed for wildly chaotic orbits evolved in two-dimensional systems. Moreover, if an orbit is wildly chaotic in two directions, but regular or much less chaotic in the third direction, one finds that moments probing the two wildly chaotic directions again resemble the moments derived from wildly chaotic ensembles in two-dimensional systems.
2. Just as the case of two-dimensional systems, there is a strong correlation between the reduced distribution  $f(Z_z, Z_b, t)$  and various moments. Suppose, e.g., that for some ensemble with two positive Lyapunov exponents, one of the reduced distributions, say  $f(z, p_z, t)$  approaches an invariant distribution much more slowly than the remaining distributions. One then finds invariably that  $\langle z \rangle$  and  $\langle p_z \rangle$  evolve towards zero more slowly than the remaining first moments, and that  $\sigma_z$  and  $\sigma_{pz}$  grow more slowly than the remaining dispersions.

Aside from these trends, three dimensions leads to several new features which reflect the possibility that the orbits can be integrable, or much less chaotic, in one configuration space direction than in the remaining two directions. The diversity of what can arise may be understood by contrasting the behaviour of ensembles comprised of orbits that are wildly chaotic in all direction, which yield moments closely resembling what is observed for unconfined chaotic orbits in two-dimensional systems, with three representative ensembles *not* wildly chaotic in all three directions, namely (1) an ensemble of completely regular orbits, (2) an ensemble of orbits which is integrable in the  $z$ -direction but wildly chaotic in the  $x$ - and  $y$ -directions, and (3) an ensemble where motion in all three directions is chaotic but the  $z$ -direction is much less chaotic than the  $x$ - and  $y$ -directions.

Figure 8, generated from the same regular ensemble used to create Fig. 7, exhibits four representative moments, namely  $\sigma_z$ ,  $\langle z \rangle$ ,  $\langle zp_y \rangle$ , and  $\langle y^2 z \rangle$ . For this and other regular ensembles, one discovers that, unlike the case in chaotic ensembles, the dispersions in all six phase space variables exhibit an overall growth which is linear, rather than exponential, in time. However, as is evident from Fig. 7 (a), this is not the whole story. The evolution of the dispersions really involves large amplitude oscillations characterised by an envelop that grows linearly in time. This sort of qualitative behaviour is also observed for other growing quantities such as  $\langle y^4 \rangle - \langle y \rangle^4$ . Indeed, one finds that all the combinations of moments which grow exponentially for a chaotic ensemble exhibit a much weaker, oscillating power law growth when computed for a regular ensemble. It would appear that an initially localised ensemble of regular orbits cannot disperse exponentially.

Analogously, one finds that the six linear moments, and all other moments which, for a chaotic ensemble, approach zero exponentially, exhibit only a modest tendency to damp. Indeed, to the extent that these moments decrease at all, that decrease is better fit by a power law than an exponential. The other obvious point is that, like the dispersions, these moments exhibit coherent oscillations. Indeed, overlaying plots of (say)  $\sigma_z$  and  $\langle z \rangle$  makes it clear that these quantities oscillate with essentially the same frequency, a fact that reflects the periodicity of the regular orbits in the ensemble. Finally, it should be noted that, in this case, not all the cross moments evolve towards zero. For example, the coherence manifested by the orbits in the ensemble would seem to imply that  $\langle zp_y \rangle$  is evolving towards a value  $\langle zp_y \rangle \approx -2.9$  rather than zero.

Figure 9 exhibits the same four moments, now computed for the wildly chaotic ensemble

used to generate Figs. 6 (b), (d), and (f), with  $a = b = 2$ , so that motion in the  $z$  direction is integrable. For this ensemble, the moments involving only  $x$ ,  $y$ ,  $p_x$ , and  $p_y$ , not shown here, all behave qualitatively like moments computed for unconfined chaotic orbits in two-dimensional potentials, such as is exhibited in Fig. 1 (a) and (b). Alternatively, as is illustrated in Fig. 9 (a) and (b), moments involving only  $z$  and/or  $p_z$  behave qualitatively like moments associated with completely regular orbits.

In some cases, moments involving both  $z$  and/or  $p_z$  and  $x$ ,  $y$ ,  $p_x$ , and/or  $p_y$  resemble moments for purely chaotic two-dimensional orbits, but in other cases they resemble results appropriate for regular orbits. That the cross moment  $\langle y^2 z \rangle$  behaves very much like the regular moment  $\langle z \rangle$  is easily understood. Because motion in the  $y$ -direction is wildly chaotic, except for very early on, there is little, if any, correlation between the values of  $y$  and  $z$  assumed by individual orbits, so that  $\langle y^2 z \rangle \approx \langle y^2 \rangle \langle z \rangle$ . However, the orbit ensemble disperses sufficiently fast in the  $y$ -direction that, within a time  $t \sim 15 - 20$ ,  $\langle y^2 \rangle$  has asymptotized towards a constant value, so that  $\langle y^2 z \rangle \propto \langle z \rangle$ . Similarly, one would expect that  $\langle zp_y \rangle \approx \langle z \rangle \langle p_y \rangle$ , which implies, in agreement with what is actually found, that this moment should die to zero exponentially like  $\langle p_y \rangle$ .

Figure 10 exhibits once again the same four moments, now computed for the ensemble used to construct Fig. 6 (a), (c), and (e), which was so chosen that, at least early on, motion in the  $z$ -direction is much less chaotic than in the  $x$ - and  $y$ -directions. Once more one finds that the moments involving only  $x$ ,  $y$ ,  $p_x$ , and  $p_y$  behave qualitatively like moments for unconfined chaotic orbits in two-dimensional potentials. The dispersions all grow exponentially, at least initially, and the linear moments decay to zero exponentially. The linear moments  $\langle z \rangle$  and  $\langle p_z \rangle$  also decrease in a fashion that is (at least) consistent with an exponential fit, although plots of these quantities show considerably more structure than what is observed for the other linear moments.

Very early on,  $\sigma_z$  and  $\sigma_{pz}$  appear to increase exponentially but, after a time  $t \sim 15$  or so, the evolution of these dispersions is better fit by a power law. Indeed, the growth of  $\sigma_z$  is so slow that one might naively conjecture that motion is regular in the  $z$ -direction. In point of fact, however, this is not so! A computation of the full spectrum of Lyapunov exponents indicates that there are two positive Lyapunov exponents; and, even more blatantly, if one evolves the orbits for a sufficiently long time (in many cases  $t > 1000$  or more), one finds that they eventually begin to act wildly chaotic in all three directions. The fact that motion in the  $z$ -direction is chaotic, albeit only moderately so, implies an absence of periodicity. This accounts for the fact that Fig. 10 (a) shows less evidence for systematic oscillations than do Figs. 8 (a) and 9 (a), as well as the fact that a plot of  $\langle zp_z \rangle$  for this ensemble is more irregular than corresponding plots for the ensembles used to generate Figs. 8 and 9. For the reason discussed in connection with Fig. 9, plots of moments like  $\langle y^2 z \rangle$  again resemble plots of  $\langle z \rangle$  and plots of  $\langle zp_y \rangle$  again resemble plots of  $\langle p_y \rangle$ .

#### 4 CONCLUSIONS AND IMPLICATIONS

The principal implication of the work described here is that, in terms of their approach towards an invariant, or near-invariant, distribution, regular and chaotic flows behave very differently. For localised ensembles of initial conditions, chaotic flows exhibit an initial exponential divergence, so that quantities like the dispersions in position and momentum increase exponentially in time. Similarly, as probed by both (i) lower order moments and (ii) coarse-grained reduced distribution functions, the ensemble will exhibit an approach towards a near-invariant distribution which proceeds exponentially in time. The time scale

associated with both the initial divergence and the ultimate approach towards a near-invariant distribution is comparable to a characteristic crossing time  $t_{cr}$ , which in turn is comparable to  $\chi^{-1}$ , where  $\chi$  represents a typical positive Lyapunov exponent. By contrast, regular ensembles exhibit an initial power law divergence and any approach towards a near-invariant distribution is typically better fit by a power law than an exponential.

In chaotic two-dimensional systems, one finds that, for a fixed potential and energy, different ensembles of unconfined chaotic orbits located far from any regular island tend to behave relatively similarly, although ensembles of confined chaotic orbits, stuck near regular islands by cantori, can behave rather differently. Moreover, the approach towards a near-invariant distribution typically proceeds at comparable rates in different directions. In many cases, this behaviour persists in three-dimensional systems. However, this is not always true. If the potential is integrable in one direction, so that chaotic orbits have only one positive Lyapunov exponent, that direction will of course behave very differently from the other two directions. However, even for a fully nonintegrable system where chaotic orbits have two positive Lyapunov exponents the approach towards a near-invariant distribution can proceed at grossly different rates in different directions.

The implication of all of this, in agreement with Merritt & Valluri (1996), is that what they call chaotic phase mixing, the process whereby an ensemble of chaotic initial conditions loses its initial coherence and approaches a near-invariant distribution, is far more efficient than regular phase mixing. If the flow were completely chaotic and especially if, as probed by short time Lyapunov exponents, the degree of chaos associated with different parts of an orbit exhibited relatively little variability, the approach towards an invariant, or near-invariant, distribution would be relatively simple to visualise and understand. However, generic potentials admit a coexistence of both regular and chaotic orbits; and, for such potentials, different parts of the same chaotic orbit can manifest grossly different amounts of chaos. One thus anticipates that, even though chaotic phase mixing will always be more efficient than regular phase mixing, it could prove a relatively complex phenomenon that manifests a significant dependence on initial conditions.

Finally it is worth noting two important caveats.

1. The operative feature that allows one to distinguish between “chaotic” and “regular” phase mixing is whether or not nearby orbits tend systematically to diverge. In principle, however, a local divergence can obtain even if the orbits are regular in the sense that, in an asymptotic  $t \rightarrow \infty$  limit, there are no positive Lyapunov exponents. All that is required is that the “local stretching number,” i.e., “short time Lyapunov exponent,” be non-zero.
2. The fact that such quantities as  $\sigma_x$  have asymptoted towards a constant nonzero value, or that moments like  $\langle p_x \rangle$  are nearly zero, does not imply the absence of any interesting subsequent evolution. All that one really expects is that any subsequent evolution will only proceed on relatively short scales. In general, one would anticipate that, for an exponentially diverging flow, an initially localised ensemble will exhibit a bulk approach towards an invariant distribution, followed by a more complicated evolution as power cascades down to progressively smaller scales, in agreement with Fig. 2 in Lynden-Bell’s (1967) original paper. A concrete example of this behaviour is exhibited in Figs. 11. The four panels here exhibit at times  $t = 2, 4, 8,$  and  $16$  the  $x$  and  $y$  coordinates of each of  $225/times225 = 50625$  unconfined chaotic orbits in the two-dimensional dihedral potential with  $E = 1.0$  which were generated by sampling the same phase space region as the ensemble used to generate Fig. 1 (a).

But what, if anything, might these conclusions imply about violent relaxation? At least

crudely, one might hope to visualise an evolution described by the collisionless Boltzmann equation as involving a collection of characteristics corresponding to orbits evolved in a specified time-dependent potential, ignoring the fact that that potential is generated self-consistently. However, to the extent that this picture is valid, one might anticipate that the efficacy with which an initial ensemble approaches an equilibrium or near-equilibrium, i.e., a time-independent, or nearly time-independent, solution to the Boltzmann equation, will depend on the degree to which the flow in the specified potential is chaotic. In particular, to the extent that the flow is chaotic, so that many/most of the orbits are characterised by positive short time Lyapunov exponents, one would expect a rapid and efficient approach towards a near-equilibrium.

Many galactic dynamicists have the intuition that “realistic” equilibrium solutions to the collisionless Boltzmann equation correspond to integrable or near-integrable potentials, which admit few if any chaotic orbits. However, even if this be true, there would seem good reason to anticipate that the time-dependent potential associated with the approach towards equilibrium will, at least initially, admit significant measures of chaotic orbits with positive short time Lyapunov exponents. Even assuming a high degree of spatial symmetry, a generic time-dependent potential  $V(\mathbf{r}, t)$  will exhibit a substantial amount of chaotic behaviour so that, at least until the time-dependence of  $V$  becomes very weak and the system is close to equilibrium, one would expect to see a significant amount of chaotic phase mixing which proceeds exponentially in time.

## ACKNOWLEDGMENTS

This work was supported in part by Los Alamos National Laboratory through the Institute of Geophysics and Planetary Physics. Some of the numerical calculations described here were facilitated by computer time provided by *IBM* through the Northeast Regional Data Center (Florida). I am grateful to Christos Siopis, Ilya Pogorelov, Donald Lynden-Bell, and Salman Habib for useful comments and interactions.

- Armbruster, D., Guckenheimer, J., Kim, S. 1989. *Phys. Lett. A* 140, 416.
- Arnold, V. I. 1964, *Russ. Math. Surveys* 18, 85.
- Aubry, S., Andre, G. 1978. in Bishop, A. R., Schneider, T. eds. *Solitons and Condensed Matter Physics*. Springer, Berlin, 264.
- Binney, J., Tremaine, S. 1987. *Galactic Dynamics*. Princeton Univ. Press, Princeton.
- Chandrasekhar, S. 1943. *Principle of Stellar Dynamics*. Univ. of Chicago Press. Chicago.
- Contopoulos, G. 1971. *AJ* 76, 147.
- Grassberger, P., Baddi, R., Politi, A. 1988, *J. Stat. Phys.* 51, 135.
- Habib, S., Kandrup, H. E., Mahon, M. E. 1996, *Phys. Rev. E* 53, 5473.
- Habib, S., Kandrup, H. E., Mahon, M. E. 1997, *ApJ* 480, 155.
- Habib, S., Kandrup, H. E., Pogorelov, I. V., Ryne, R. 1998, in preparation.
- Kandrup, H. E. 1998, *ApJ* 500, 120.
- Kandrup, H. E. 1998, *Ann. N. Y. Acad. Sci.*, in press.
- Kandrup, H. E., Mahon, M. E. 1994, *Phys. Rev. E* 49, 3735.
- Lichtenberg, A. J., Lieberman, M. A. 1992, *Regular and Chaotic Dynamics*. Springer, Berlin.
- Lynden-Bell, D. 1967, *MNRAS* 136, 101.
- MacKay, R. S., Meiss, J. D., Percival, I. C. 1984, *Phys. Rev. Lett.* 52, 697.
- Mahon, M. E., Abernathy, R. A., Bradley, B. O., Kandrup, H. E. 1995. *MNRAS* 275, 443.
- Mather, J. N. 1982, *Topology* 21, 45.
- Merritt, D., Valluri, M. 1996. *ApJ* 471, 82.
- Morrison, P. J. 1980, *Phys. Lett. A* 80, 383.
- Pogorelov, I., Kandrup, H. E. 1998, in preparation.
- Toda, M. 1967. *J. Phys. Soc. Japan* 22, 431.
- Wolf, A., Swift, J. Swinney, H., Vastano, J. 1985, *Physica D* 16, 285.

## FIGURE CAPTIONS

Figure 1. (a) The  $L^2$  (upper boldface curve) and  $L^1$  (lower curve) distance  $Df(x, y, t)$  between  $f(x, y, t)$  and a near-invariant  $f_{niv}(x, y)$  computed for an ensemble of 6561 unconfined orbits with  $E = 1.0$  evolved in the dihedral potential (4). (b) The same for an ensemble of 6561 unconfined chaotic orbits with  $E = 6.0$ . (c)  $Df(xp_x, t)$  for a different ensemble of 6561 unconfined chaotic orbits with  $E = 6.0$ . (d)  $Df(y, p_y, t)$  for the ensemble used to generate (c). (e)  $Df(x, y, t)$  for an ensemble of 6561 orbits with  $E = 4.0$ . (f)  $Df(y, p_y, t)$  for the ensemble used to generate (e).

Figure 2. The  $L^2$ - (upper boldface curve) and  $L^1$ - (lower curve) distances  $D\tilde{f}(x, y, t)$  for the ensemble used to construct Fig. 1(a), now considering a coarse-grained  $\tilde{f}(x, y, t)$  which averages over a variable number  $k$  of successive time steps separated by  $\Delta t = 0.5$ . (a)  $k = 3$ . (b)  $k = 15$ .

Figure 3. The mean  $L^1$  convergence rate  $\Lambda_{L1}$  for individual snapshots (dot-dashed curve), the mean  $L^2$  convergence rate  $\Lambda_{L2}$  averaging over between five and 25 time steps (triple-dot-dashed curve), the mean  $L^2$  convergence rate for individual snapshots (dashed curve), and  $0.5\bar{\chi}$  (solid curve), with  $\bar{\chi}$  the mean value of the largest Lyapunov exponent, for ensembles of unconfined chaotic orbits with variable energy  $E$ . The error bars were generated by averaging over several different ensembles at each energy.

Figure 4. Logarithmic plots of several moments computed for the ensemble of unconfined chaotic orbits with  $E = 1.0$  evolved in the dihedral potential used to generate Fig. 1. (a)  $\ln |\langle x \rangle|$ . (b)  $\ln |\langle xy \rangle|$ . (c)  $\ln |\langle p_x p_y \rangle|$ . (d)  $\ln |\langle xp_x \rangle|$ . (e)  $\ln |\langle xp_y \rangle|$ . (f)  $\ln (\langle x^4 \rangle - 2\langle x^2 \rangle^2)$

Figure 5. Logarithmic plots of dispersions computed for the ensemble used to generate Fig. 7. (a)  $\ln \sigma_x$ . (b)  $\ln \sigma_{px}$ .

Figure 6.  $L^2$  (upper boldface curve) and  $L^1$  (lower curve) distances  $Df(t)$  computed for an ensemble of 6561 unconfined orbits with  $E = 6.0$  evolved in the three-dimensional potential with (i)  $a = b = 1$  and (ii)  $a = b = 2$ . (a)  $Df(x, y, t)$  for the ensemble with  $a = b = 1$ . (b)  $Df(x, y, t)$  for the ensemble with  $a = b = 2$ . (c)  $Df(z, p_x, t)$  for the ensemble with  $a = b = 1$ . (d)  $Df(z, p_x, t)$  for the ensemble with  $a = b = 2$ . (e)  $Df(z, p_z, t)$  for the ensemble with  $a = b = 1$ . (f)  $Df(z, p_z, t)$  for the ensemble with  $a = b = 2$ .

Figure 7.  $L^2$  (upper boldface curve) and  $L^1$  (lower curve) distances  $Df(t)$  computed for an ensemble of 6561 regular orbits with  $E = 4.0$  evolved in the three-dimensional potential (7) with  $a = b = 1$ . (a)  $Df(x, y, t)$ . (b)  $Df(x, p_y, t)$ .

Figure 8. Four different moments computed for an ensemble of 6561 regular orbits with  $E = 4.0$ , evolved in the three-dimensional potential (7) with  $a = b = 1$ . (a) The dispersion  $\sigma_z$ . (b).  $\langle z \rangle$ . (c)  $\langle zp_y \rangle$ . (d)  $\langle y^2 z \rangle$ .

Figure 9. Four different moments computed for an ensemble of 6561 chaotic orbits with  $E = 6.0$ , evolved in the three-dimensional potential (7) with  $a = b = 2$ . (a) The dispersion  $\sigma_z$ . (b).  $\langle z \rangle$ . (c)  $\langle zp_y \rangle$ . (d)  $\langle y^2 z \rangle$ .

Figure 10. Four different moments computed for an ensemble of 6561 chaotic orbits with  $E = 6.0$ , evolved in the three-dimensional potential (7) with  $a = b = 1$ . Initial conditions were chosen so that the orbit are initially much less chaotic in the  $z$ -direction than the  $x$ - and  $y$ -directions. (a) The dispersion  $\sigma_z$ . (b).  $\langle z \rangle$ . (c)  $\langle zp_y \rangle$ . (d)  $\langle y^2 z \rangle$ .

Figure 11. The  $x$  and  $y$  coordinates of 50625 unconfined chaotic orbits evolved in the two-dimensional dihedral potential with  $E = 1.0$ , generated from initial conditions that sampled the same phase space region as did the ensemble used to produce Fig. 1 (a). (a) Time  $t = 2$ . (b)  $t = 4$ . (c)  $t = 8$ . (d)  $t = 16$ .

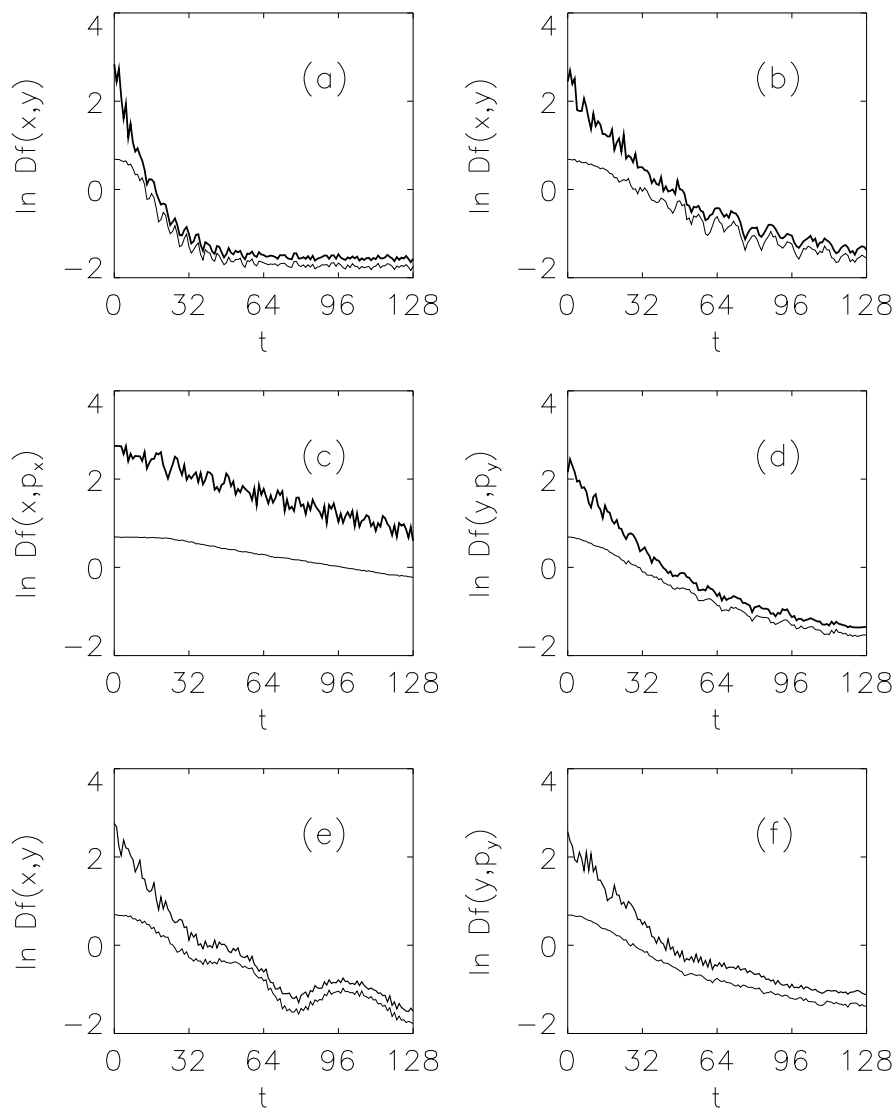


Figure 1.

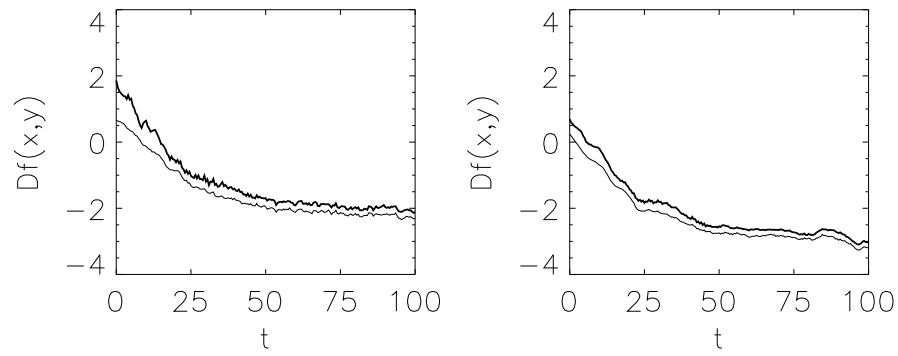


Figure 2.

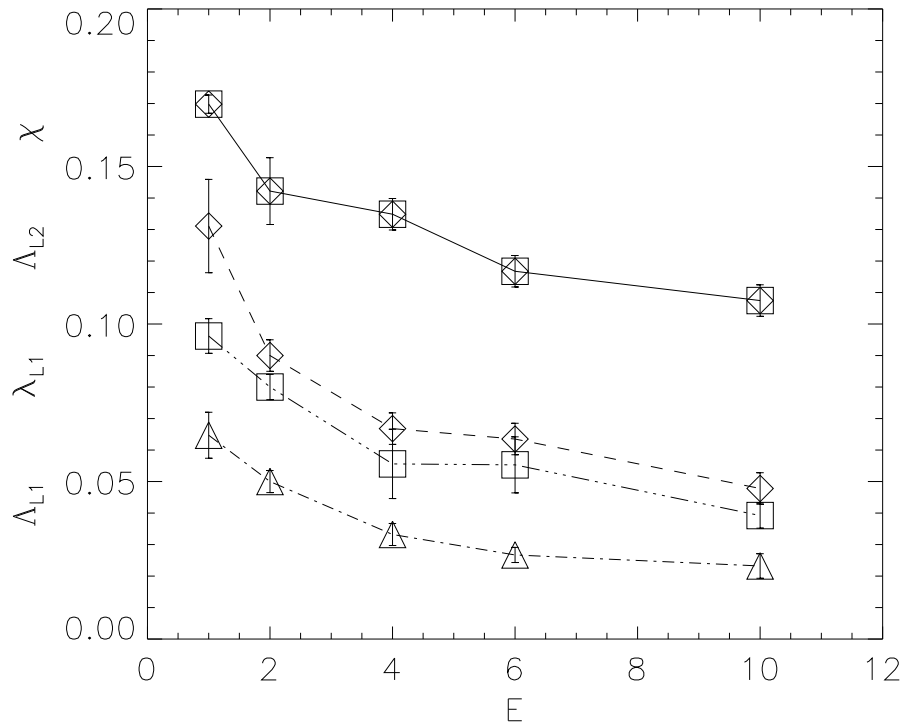


Figure 3.

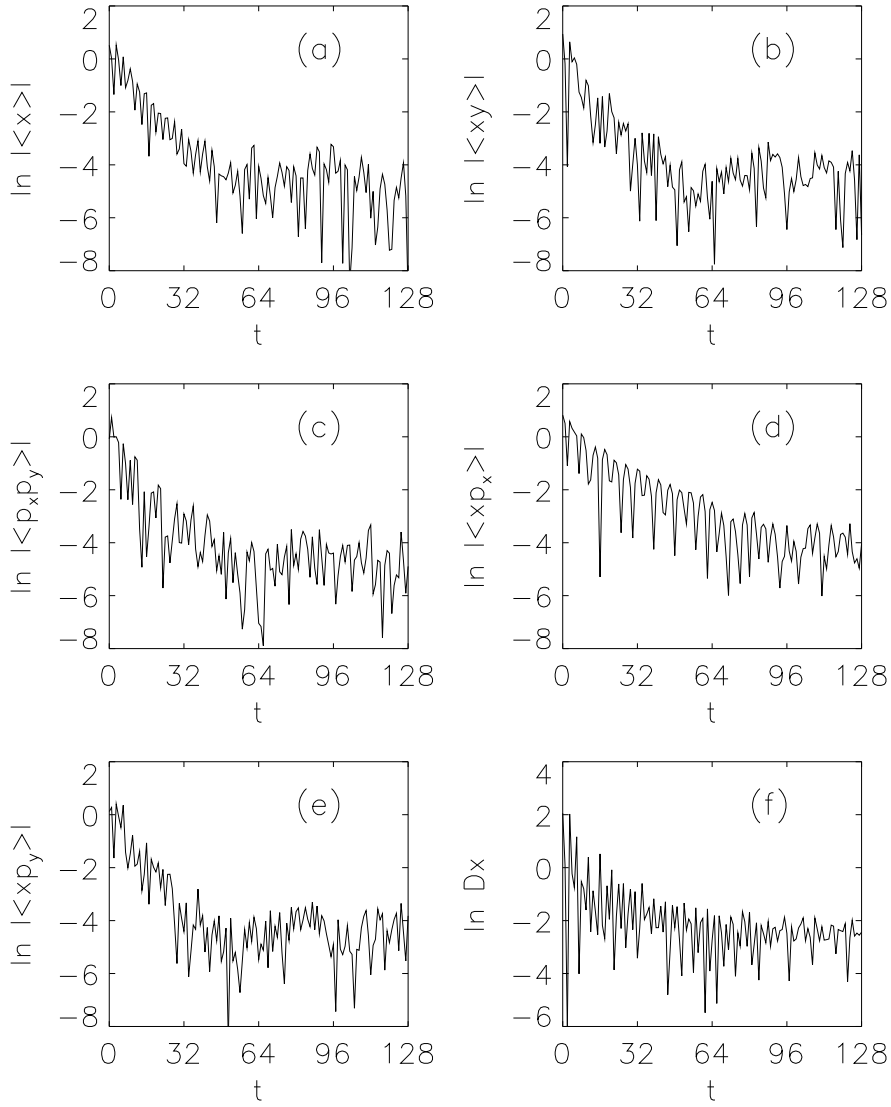


Figure 4.

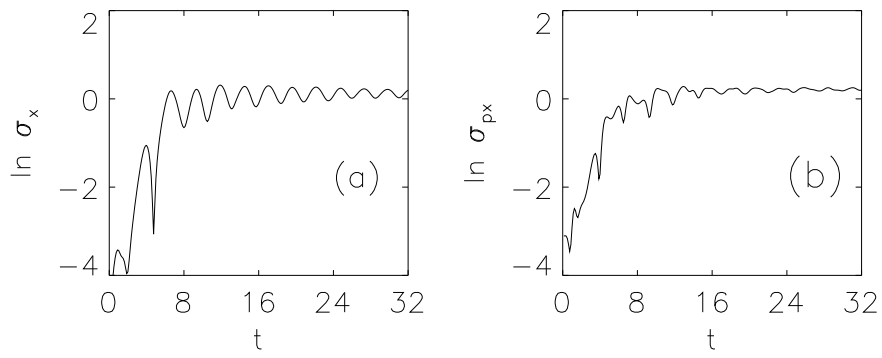


Figure 5.

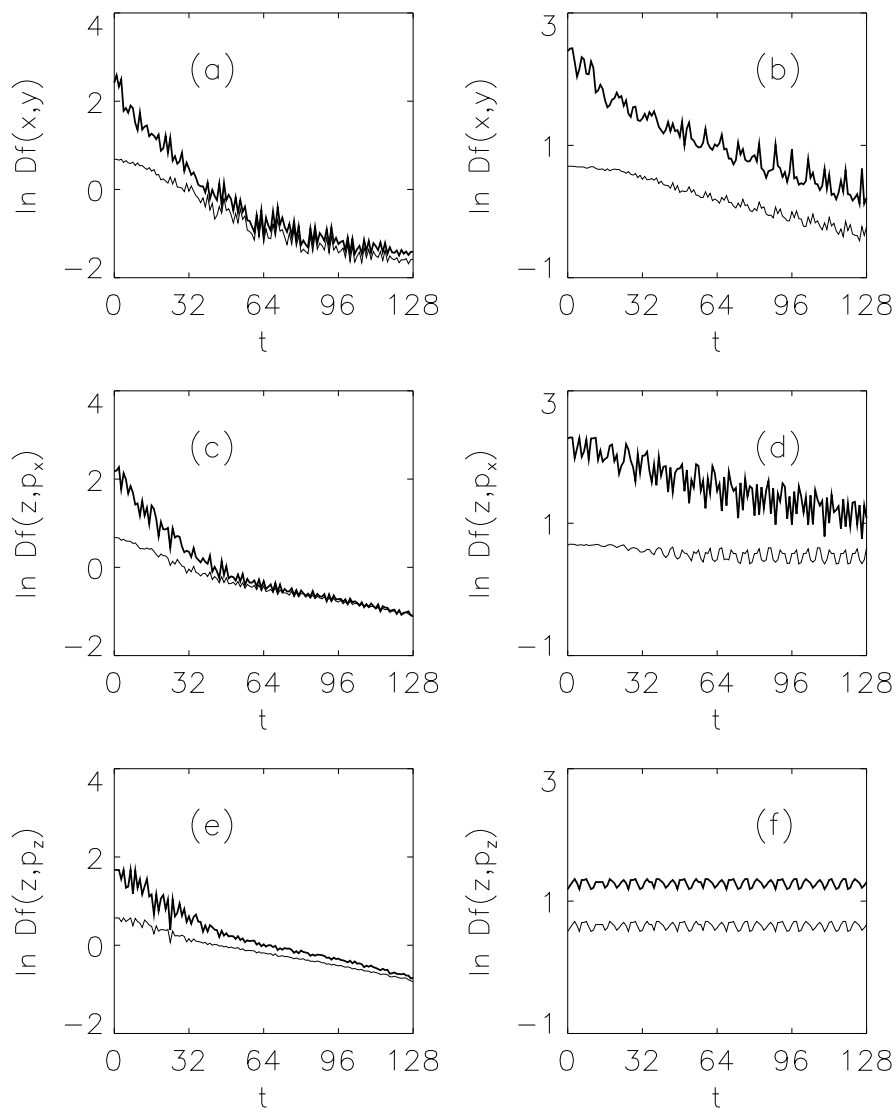


Figure 6.

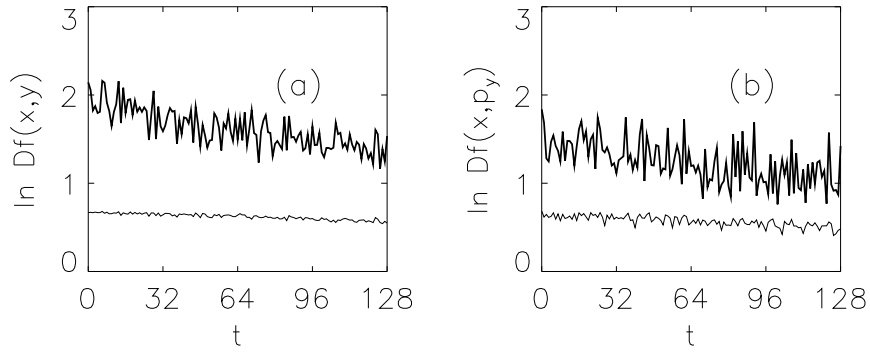


Figure 7.

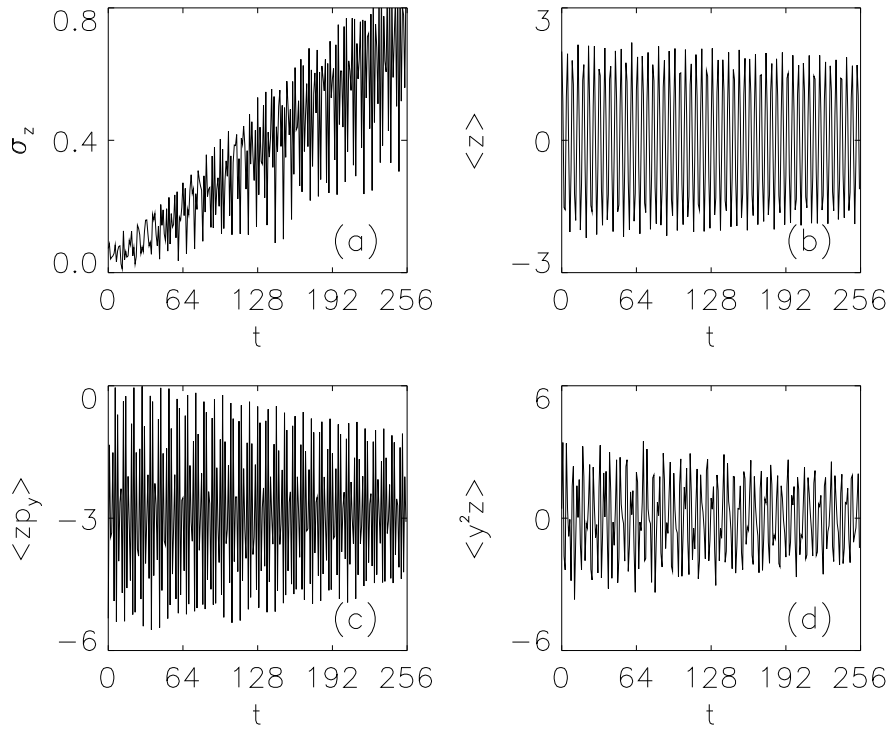


Figure 8.

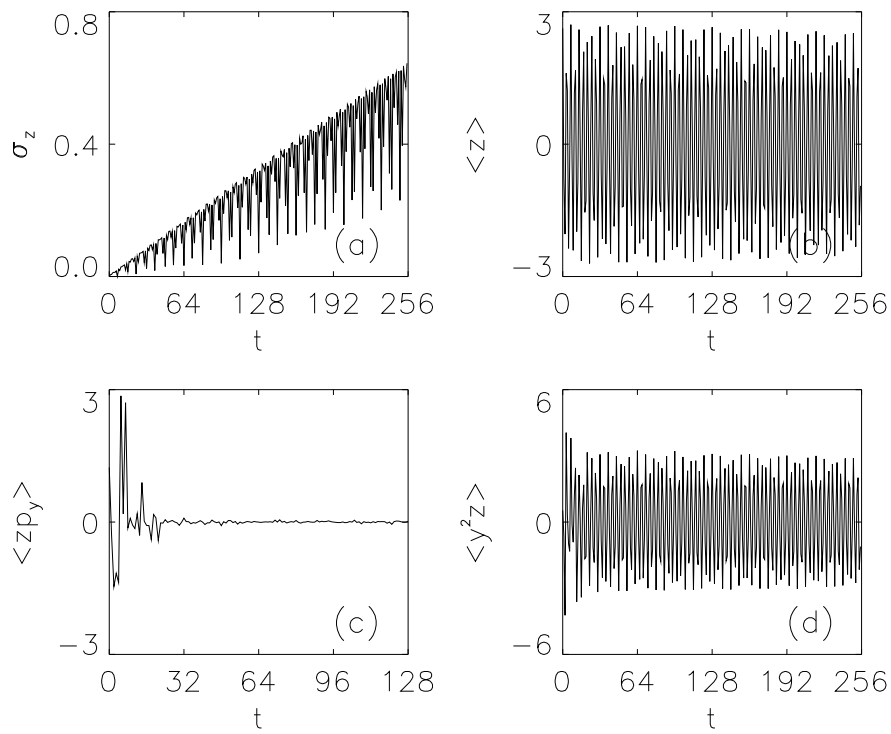


Figure 9.

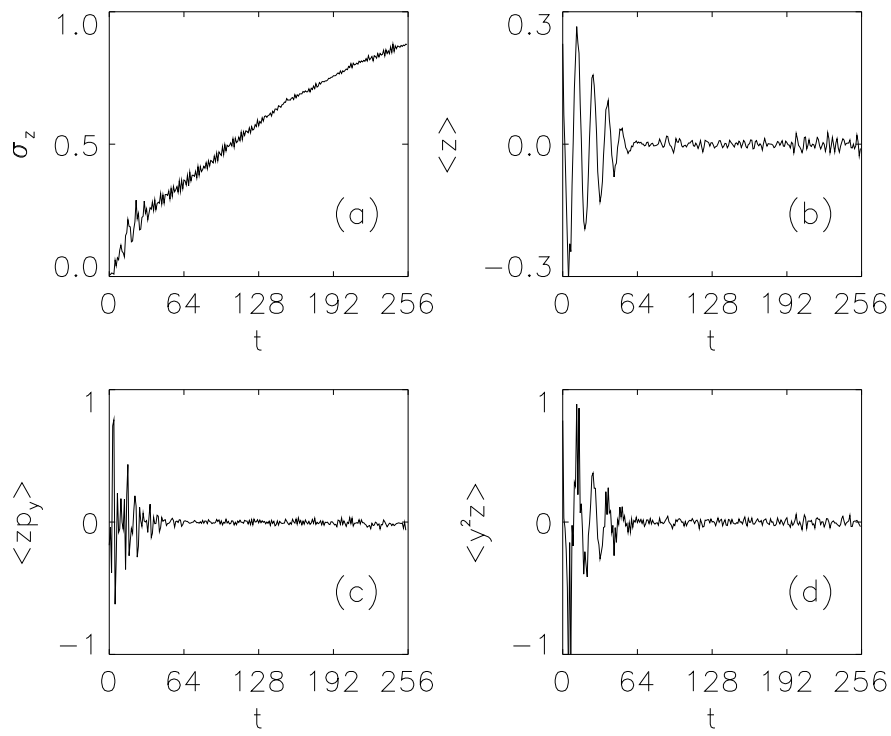


Figure 10.

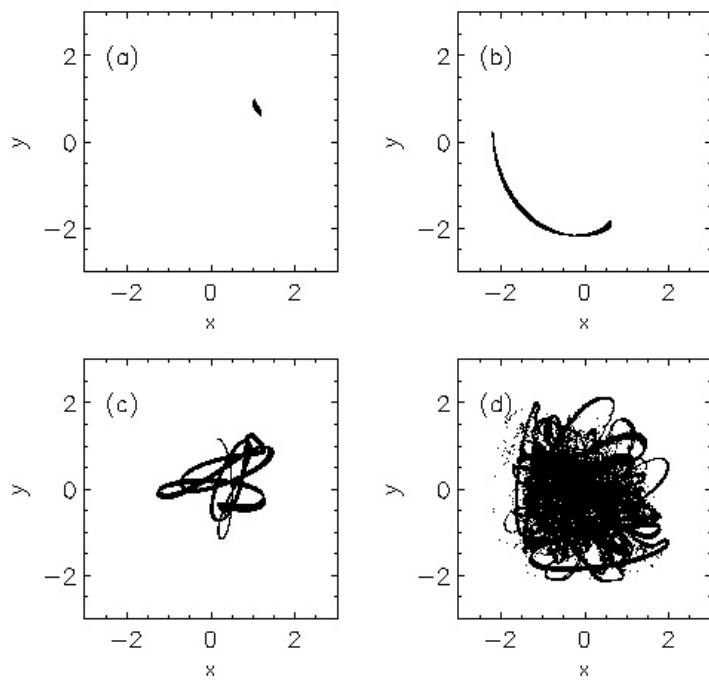


Figure 11.